J. F. Flavenot and N. Skalli**

A Comparison of Multiaxial Fatigue Criteria Incorporating Residual Stress Effects

REFERENCE Flavenot, J. F. and Skalli, N., **A comparison of multiaxial fatigue criteria, incorporating residual stress effects**, *Biaxial and Multiaxial Fatigue*, EGF 3 (Edited by M. W. Brown and K. J. Miller), 1989, Mechanical Engineering Publications, London, pp. 437–457.

ABSTRACT Any attempt to account for residual stresses when asssessing fatigue strength leads to the question of choosing an appropriate design criterion. The mode of fatigue loading of a component or structure may be monoaxial, but residual stresses are always multiaxial. If design engineers need to evaluate the fatigue strength of an artefact that has a residual stress, they must be able to provide for all types of stress in their calculations.

Fatigue testing and the measurement of the stabilised residual stress in induction-hardened components and ground samples have shown that the von Mises criterion currently used elsewhere does not describe the behaviour of a material with sufficient accuracy.

Crossland's criterion, which is derived from von Mises' criterion, and which takes into account hydrostatic pressure, and the Dang Van criterion (based on maximum alternate shear and hydrostatic pressure) provide a better correlation to results obtained by experiment.

Introduction

All methods of manufacture introduce residual stresses in components and mechanical structures, and can considerably modify performance in service; in particular their resistance to fatigue. These fatigue stresses will be superimposed on the load applied to the component and thus modify the stress distribution, especially in the surface layers where cracking due to fatigue is most frequently initiated.

Taking into account residual stress when estimating fatigue behaviour poses the problem of analysing components subjected to multi-axial stress. The state of stress resulting from applied loads may be uniaxial, but the state of a residual stress pattern is always multiaxial. Where residual stresses are present in a component, the design engineer needs a multiaxial fatigue criterion to be able to evaluate the fatigue resistance of the component.

In this analysis several criteria of multiaxial fatigue are compared by using results from fatigue tests and measurements of residual stress in an induction-hardened XC42 steel cylindrical bar, and also from ground 42CD4 steel plane specimens. The results underline the importance of choosing criteria which involve the role of hydrostatic pressure and the amplitude of maximum or octahedral shear stress when estimating the fatigue behaviour of materials in which stresses are present.

* CETIM, 52 Avenue Félix Louat, 60304–Senlis, France.

Notation

σ_a	Stress amplitude (uniaxial fatigue loading)
σ_m	Mean stress of the fatigue loading (uniaxial loading)
σ_D	Fatigue strength of the materials for $\sigma_m = 0$
σ_R	Residual stress
σ_{Rl}	Longitudinal residual stress
σ_{Rt}	Tangential or transverse residual stress
$\sigma_1, \sigma_2, \sigma_3$	Principal stresses due to multiaxial loading
$\sigma_{1m}, \sigma_{2m}, \sigma_{3m}$	Mean principal stresses due to multiaxial fatigue loading
$\sigma_{1a}, \sigma_{2a}, \sigma_{3a}$	Principal stresses amplitudes due to multiaxial fatigue loading
$\sigma_{eq,m}$	Tensile equivalent mean stress (von Mises' criterion)
$\sigma_{eq,a}$	Tensile equivalent stress amplitude (von Mises' criterion)
σ_n	Normal stress (normal to the plane of maximum shear)
$\sigma_{at,p}$	Normal octahedral stress (normal to the octahedral shear plane)
p_m	Mean value of the hydrostatic pressure (or hydrostatic stress) during fatigue loading
p_{max}	Maximum hydrostatic pressure
τ_a	Shear stress amplitude
$\tau_{oct,a}$	Octahedral shear stress amplitude
$\alpha, \alpha', \beta, \beta'$	Material constants

The importance of residual stresses in fatigue

According to the size of the three-dimensional component concerned, several types of residual stress can be distinguished. Macroscopic or first order stresses give rise to bulk strains and act on the component as a whole or on a significant part of its volume. Second order residual stresses act at the level of the metal grains, and the third order residual stresses concern the crystal structure. These three types of stress are, of course, interactive, and so modify the behaviour of the material. However, it is the macroscopic stresses that are of interest to the engineer, because they have a direct influence on the strains and the strength of the mechanical part.

The nature of macroscopic residual stresses is such that one can apply the fundamental equations of elasticity and, in particular, the theory of superposition. Consequently, when a component is subjected to a residual stress field, σ_R, and a working stress, σ_S, it will in fact be subjected to a stress of $\sigma_R + \sigma_S$. For this reason, it has been normal practice to quantify the effect of the residual stresses in fatigue using a Haigh or Goodman chart, in which σ_m, the mean stress in a fatigue cycle, is replaced by the mean stresses $\sigma'_m = \sigma_m + \sigma_R$, see Fig. 1.

Numerous test results have been treated using relationships such as

$$\sigma_a = \sigma_D - \alpha(\sigma_R + \sigma_m) \tag{1}$$

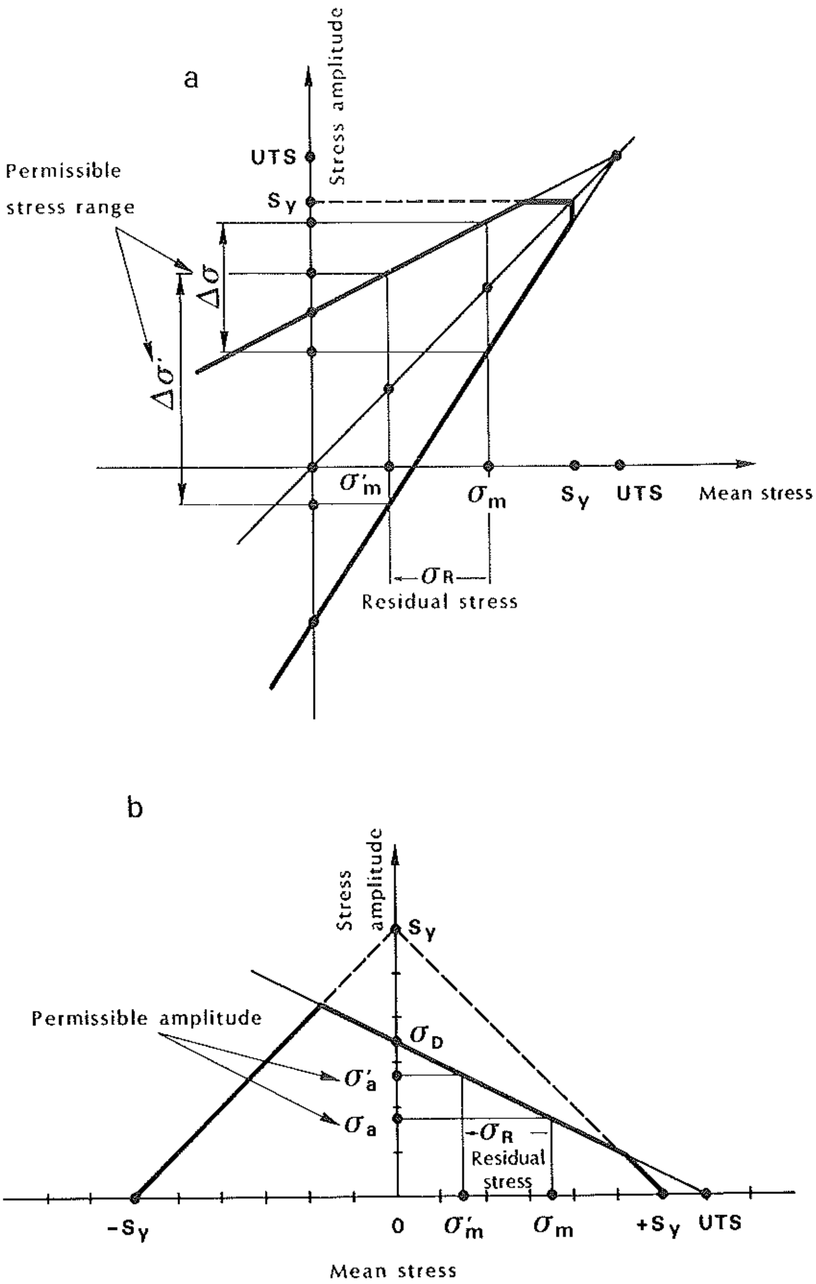

Fig 1 Use of (a) Goodman or (b) Haigh diagrams to estimate resistance to fatigue in the presence of residual stress

where

σ_a = amplitude of stresses allowed
σ_m = mean stress due to fatigue loading
σ_R = residual stress
σ_D = fatigue strength of the material for $\sigma_m = \sigma_R = 0$
α = material constant

Although this may provide a very simple means of predicting the effect of residual stress on fatigue strength, two important aspects are neglected: the effect of stress-relieving (or cyclic stress relaxation), and the multiaxial nature of the residual stresses.

It is accepted that residual stresses decrease when the material is subjected to cyclic loading, and stress-relieving may be total or partial, depending on the applied load, the type of treatment which induced the residual stresses, and the nature of the material. Most of the time, stress-relieving is neglected by those using fatigue charts or a relationship of the type of equation (1), and it is the value of the residual stresses after manufacture and before fatigue which is used in the calculation. Therefore, the values of coefficient α for various materials and processes found in references (1)–(4) do in fact incorporate the effect of relieving residual stresses. This can lead to considerable error when one attempts to generalize this method of calculation for loads, materials, or processes for which the coefficient has not previously been determined by experiment.

In fact, taking into account the residual stress in a calculation necessarily implies the determination of the values of the stabilised residual stresses either by measurement on components having already been subjected to fatigue loading, or by calculation, if adequate models are available.

Besides, the use of fatigue charts of the Haigh or Goodman type (see ISO/R373–1964 recommendation) only takes into account the residual stress parallel to the fatigue stress. However, in practice, a simple uniaxial residual stress does not exist. All manufacturing processes will in fact produce a stress field which is biaxial at the surface of the component and triaxial below the surface layer. One should therefore take into account in fatigue calculations a biaxial or triaxial state of stress according to the possible site of cracking, the biaxial stress field of the surface and the triaxial pattern of stress of the surface layer. This problem raises the question of selecting a multiaxial fatigue criterion, and shows that the simplified approach using fatigue charts can only be an approximation.

This paper presents work carried out in an attempt to validate multiaxial fatigue criteria from results obtained from fatigue testing of components where residual stresses are present.

Experimental results

A comparison is made between the best known criteria for multi-axial fatigue using data from two series of experimental results, including fatigue testing and residual stress measurements on induction-hardened XC42 steel cylindrical specimens and on flat ground specimens of a 42CD4 AFNOR steel.

Induction-hardened cylindrical specimens of XC42 steel

Fatigue tests were performed in repeated plane bending on induction-hardened 36 mm diameter XC42 steel cylindrical bars. In order to avoid any effect of surface finish, the test specimens were finely turned to a R_t value in the range 5–7 μm before treatment.

Quenching after induction heating induces very high compressive residual surface stresses due to a volume increase of the martensitic structure with respect to the ferrite–pearlite structure obtained in the annealed state. In the cylindrical induction-hardened test specimens, the surface residual stresses generally give rise to a tangential residual stress equal to, or slightly higher than the axial residual stress (see Fig. 2). The thickness of material subjected to

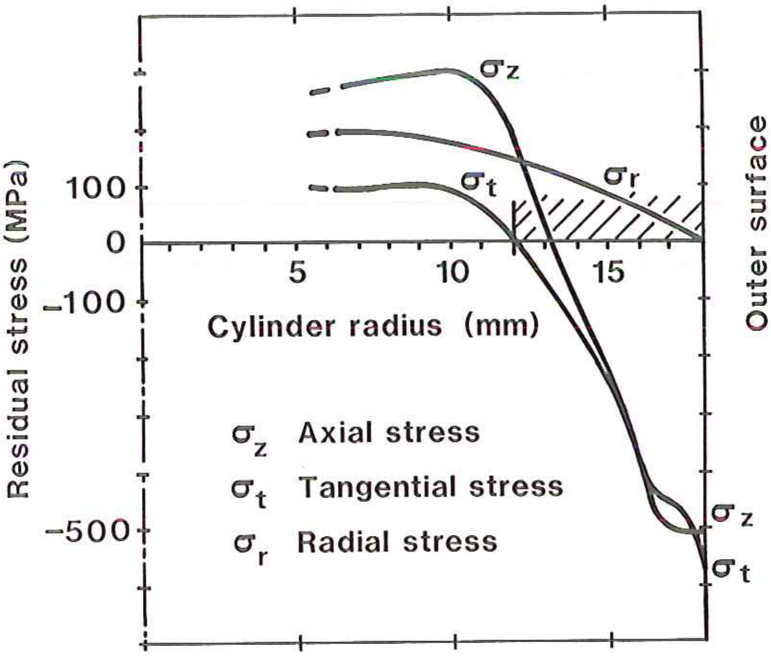

Fig 2 Example of the residual stress distribution obtained after induction-hardening at low frequency. Stress measurement using Sachs method. Surface hardness 54HRC, hardened depth 2.8 mm, XC42 steel

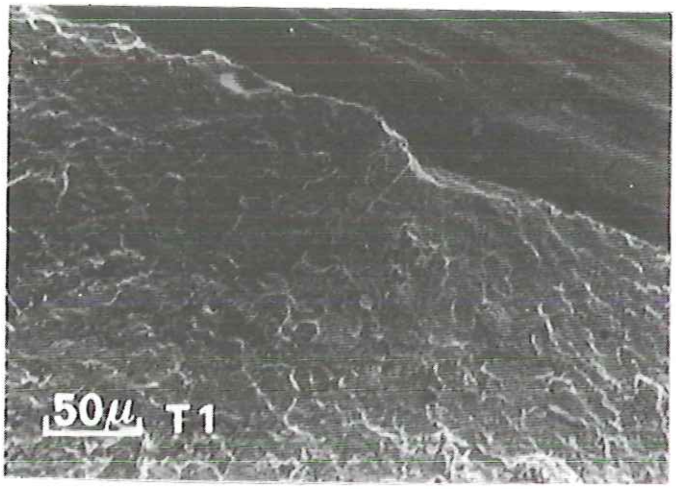

a

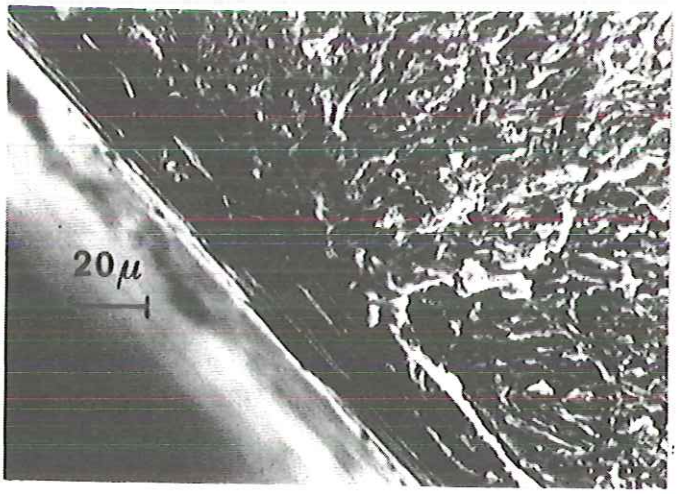

Fig 3 Photomicrographs of fatigue crack initiation: (a) induction hardened cylindrical bar (XC42 steel); (b) severely ground flat test pieces (42CD4 steel)

compressive residual stresses is of the same order as the thickness of the hardened layer (**5**).

Measurements of residual stresses were carried out on test specimens subjected to $5 \cdot 10^6$ fatigue cycles at a load corresponding to the fatigue limit for the treatment considered. Measurements were made at the surface where fatigue cracking occurred (see Fig. 3). In this case, the state of stress at the surface governs the fatigue strength. Measurements were made by X-ray

Table 1 Fatigue and hardness characteristics of four different types of surface treatments (XC42 carbon steel)

	Type of hardening and hardened depth (45HRC)	*Surface hardness HRC*	*Repeated bending fatigue limit (MPa)*		*Stabilized residual stresses (MPa)*	
			σ_m	σ_a	σ_{Rl}	σ_{Rt}
A	Induction 2.7 mm	55–56	596	584	−128 −243	−468 −571
B	Induction 4.2 mm	55–56	623	610	−273 −341	−583 −676
C	Induction 4.7 mm	54–59	670	660	−655	−603
D	Water quenched 3.5 mm	60–61	750	750	−863 −777	−1123 −1156

diffraction. On each test specimen, values of σ_{Rl} (longitudinal or axial residual stress) and σ_{Rt} (tangential residual stress) were measured. The results obtained for the four different heat-treatments considered are shown in Table 1.

Calculating fatigue strength with due consideration to the residual stress pattern requires knowledge of the fatigue strength of the surface layer in the absence of residual stresses. For this reason, fatigue tests were carried out by repeated tensile loading on XC42 steel cylindrical specimens, homogeneously hardened to a value of 52HRC close to the value (54-56HRC) obtained by induction-hardening.

By means of tensile testing, the ultimate strength of the steel homogeneously treated was determined. Based on these results, a Haigh fatigue chart for the metal without residual stresses was plotted. This chart probably illustrates the approximate behaviour in fatigue of the induction-hardened layer without residual stresses. For this chart, the value for the stress amplitude with respect to the mean stress is given at the fatigue limit by the linear relation

$$\sigma_a = 715 - 0.33\sigma_m \qquad (2)$$

where stresses are in MPa.

Ground flat specimens of 42CD4 steel

Fatigue tests under various conditions were performed by repeated plane bending of flat ground test specimens 5 mm thick in 42CD4 steel quenched and tempered to 40 HRC hardness (UTS = 1250 MPa). It is generally accepted that grinding generates heat and residual tensile stresses in the surface layers of the metal. Under severe conditions of machining, the stress level may be extremely high (6). Generally speaking, the transverse residual stress with respect to the

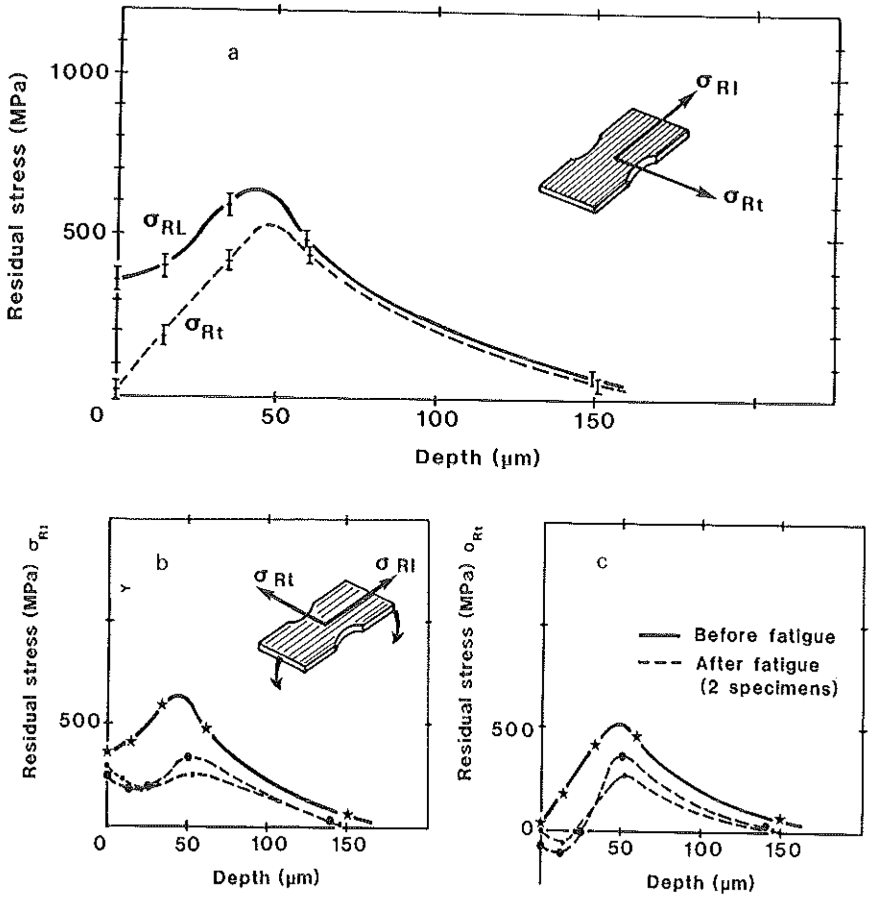

Fig 4 Residual stress distribution for severely ground 42CD4 steel (plane bending test pieces): (a) longitudinal and transverse residual stress before fatigue testing; (b) relief of the longitudinal residual stress by fatigue; (c) relief of the transverse residual stress by fatigue

direction of grinding is of the same order but slightly less than the longitudinal residual stress, see Fig. 4(a).

Measurements of residual stresses were carried out by X-ray diffraction on test specimens subjected to $5 \cdot 10^6$ fatigue cycles at a load corresponding to the fatigue limit for the treatment considered. On examination of the specimens, it was not possible to clearly determine whether cracking due to fatigue started at the surface or slightly below (see Fig. 3). The peak value of the tensile stress, rather than the value of the residual stresses at the surface, was used for the calculation of the various criteria. In the case of grinding, the steep gradient of residual stresses makes it desirable to use the peak value of the residual stresses. The results obtained are given in Table 2.

Table 2 Specimen preparation, residual stress, and fatigue data for ground 42CD4 steel

Grinding type	*Mark*	*Type and Young's modulus of wheel*	*Finishing condition*	*Roughness* Rt *(μm)*	*Fatigue limit (MPa)*	*Surface stabilized residual stresses (MPa)* σ_{Rl}	σ_{Rt}
Soft longitudinal	AL	Soft A46HV $E = 33.3$ KN/mm^2	Depth of cut 5 μm	7.4	762	+113	−157
Soft transverse	AT			7.5	690	+125	−200
Medium longitudinal	CL	Medium A48KV $E = 41.4$ KN/mm^2	Depth of cut 15 μm	8.7	751	+247 +233	−13 −122
Severe longitudinal	DL	Hard A3605V $E = 57.8$ KN/mm^2	Depth of cut 30 μm	11.9	564	+337 +250 +309	+376 +272 +311
Severe transverse	DT			11.4	520	+361 +350 +340	+260 +285 +308

In the above series of experiments, the same grinding conditions were applied either parallel to or transverse to the longitudinal axis of the test specimens, with the purpose of differentiating the effects of surface finish and residual stresses with respect to the fatigue strength. In the case of longitudinal grinding, the traces due to grinding are in fact parallel with the direction of the fatigue stress, and the surface finish has no effect on fatigue resistance. However, transverse grinding gives traces perpendicular to the fatigue stress, and the fatigue limit decreases as a result of this rougher surface.

Measurements of residual stresses were also carried out prior to fatigue testing in order to evaluate the degree of relief of the grinding residual stress. As an example, Fig. 4(b) shows the results obtained for the case of severe grinding. It can be noted that for the residual stress parallel to the fatigue stress, stress-relieving is higher than that for the residual stress which is perpendicular to the fatigue stress. This result appears to be general, and also has been noted in the case of induction-hardened cylindrical specimens.

Finally, in order to have a reference fatigue chart for 42CD4 steel without residual stresses, rotating bending fatigue tests were carried out on cylindrical bars which had been subjected to slight longitudinal grinding and assumed to have no residual stresses. On the basis of this result, an approximate reference fatigue chart was obtained which could be expressed by the following linear equation

$$\sigma_a = 490 - 0.4\sigma_m \tag{3}$$

where stresses are in MPa.

Treatment of experimental results with respect to multiaxial fatigue criteria

To compare and to validate various methods of calculation, values for the stabilised residual stresses measured after fatigue testing were introduced into various criteria as mean stresses. The results obtained were then compared with a reference fatigue chart (Haigh or Goodman), when available. In the absence of such a chart, only the validity of the criterion could be investigated by examining the correlation between the experimental and the calculated results.

Utilisation of the Haigh or Goodman chart

In the traditional method, when taking into account the residual stresses with a Haigh or Goodman fatigue chart, only the residual stress parallel to the direction of fatigue stress is accounted for, whereas the transverse residual stress is totally neglected.

The calculation is carried out by simply plotting on the σ_a vs σ_m fatigue chart the points obtained by experiment, which are defined by the coordinates σ_a (fatigue stress at the fatigue limit) and σ_m (mean stress of the fatigue test, to which has been added the residual stress parallel to the cyclic stress).

The results obtained are plotted on Fig. 5. At first sight, it is obvious that the method works correctly in the case of induction-hardening, but not in the case of grinding. Therefore, this method cannot be generalised, and cannot be validated unless it has been justified beforehand, by means of experiment, for the material, the manufacturing process, and the load.

The Kiocecioglu criterion

Kiocecioglu (7) has suggested an extrapolation of von Mises' criterion of plasticity to the fatigue limit under multiaxial stresses. This approach is justified by the fact that, as in the case for plastic strain, the mechanism for initiating fatigue cracking resides in the shear stress on specific crystallographic planes. The von Mises criterion involves the the effect of octahedral shear (shear stress acting in a plane equally inclined with respect to the three principal axes) and, as a result, is characteristic of a kind of average shear acting on the differently orientated grains of metal.

From a complex state of stress, the von Mises criterion allows for the calculation of an equivalent tensile stress. Kocecioglu, therefore, proposed the

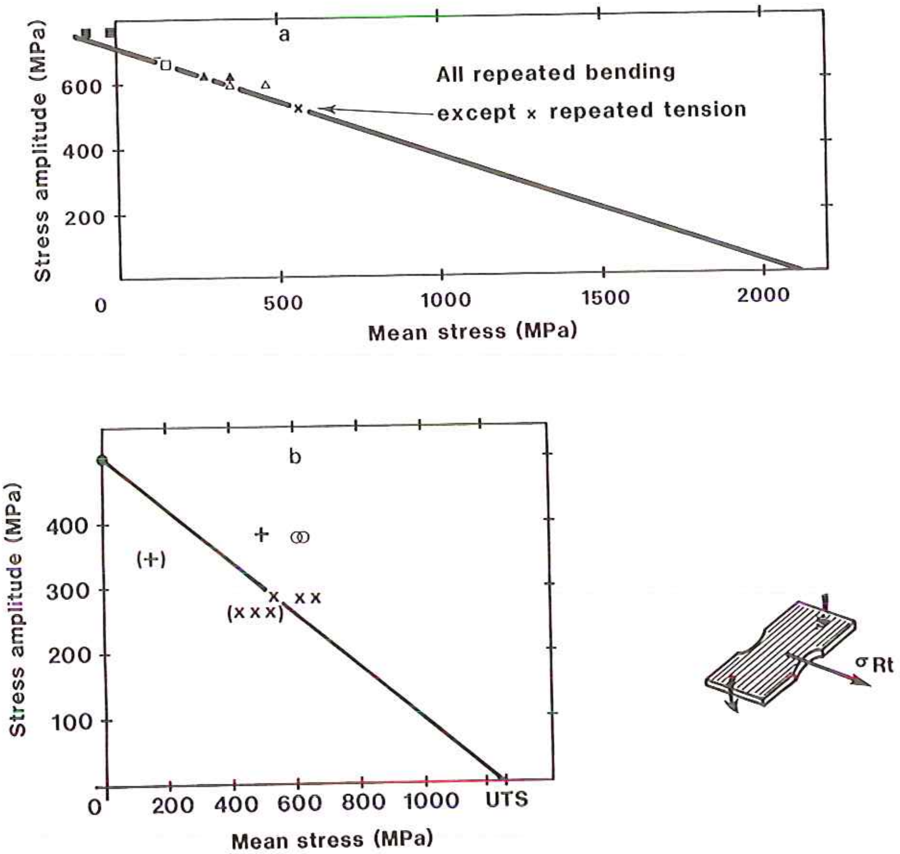

Fig 5 Utilisation of the Haigh diagram, neglecting the effect of transverse residual stress, with respect to stress due to repeated bending fatigue: (a) induction hardened cylindrical bars (XC42 steel); (b) ground material (42CD4 steel)

application of this calculation to the alternating stress and to the mean stress. In the case of fatigue cracking initiated at the surface, the state of stress is biaxial, and the equivalent stresses can be calculated from the relationships

$$\sigma_{eq,m} = (\sigma_{1m}^2 + \sigma_{2m}^2 - \sigma_{1m} \cdot \sigma_{2m})^{1/2} \quad (4)$$

$$\sigma_{eq,a} = (\sigma_{1a}^2 + \sigma_{2a}^2 - \sigma_{1a} \cdot \sigma_{2a})^{1/2} \quad (5)$$

where σ_m, the mean stress due to the fatigue load, and σ_{Rl} and σ_{Rt}, the longitudinal and transverse residual stresses with respect to the orientation of the fatigue load, are introduced into equation (4) through the definition of σ_{1m} and σ_{2m}, the two mean principal stresses, which, for the plane bending tests on XC42 cylindrical bars, give

$$\sigma_{1m} = \sigma_m + \sigma_{Rl} \tag{6}$$

$$\sigma_{2m} = \sigma_{Rt} \tag{7}$$

For each experimental result considered, both $\sigma_{eq,m}$ and $\sigma_{eq,a}$ were plotted on the Haigh reference chart. The results, in Fig. 6 show that the points which represent these results are not on the reference curve. Therefore, extrapolation of the von Mises criterion to fatigue in the presence of mean or residual stresses does not appear to be justified.

The Sines criterion

On the basis of the statement that a mean torsional stress only has a minor effect on fatigue strength, Sines (8) has suggested to take into account the effect of the mean hydrostatic pressure. This criterion includes the octahedral shear $\tau_{oct,a}$ and the hydrostatic pressure p_m in a linear equation of the form

$$\tau_{oct,a} + \alpha \cdot P_m = \beta \tag{8}$$

The hydrostatic pressure is in fact the normal octahedral stress representing the stress acting perpendicularly on the octahedral plane as defined above. It is equal to one third of the sume of the principal stresses

$$p = \sigma_{oct} = (\sigma_1 + \sigma_2 + \sigma_3)/3$$

The equivalent stress, as interpreted by von Mises, is related to the octahedral shear, and equation (8) can be rewritten

$$\sigma_{eq,a}(\text{Mises}) + \alpha' \cdot p_m = \beta' \tag{9}$$

In the case of the fatigue tests considered here, $\sigma_{eq,a}$ is obtained from equation (5) in which σ_{1a} and σ_{2a} represent the principal stresses. The mean hydrostatic pressure will be equal to one third of the sum of the mean and the residual stresses; for example, for the XC42 cylindrical bars

$$p_m = (\sigma_m + \sigma_{Rl} + \sigma_{Rt})/3 \tag{10}$$

Therefore, all $\sigma_{eq,a}$ and p_m values corresponding to the experimental results can be plotted on the $\sigma_{eq,a}$ vs p_m chart, and thus compared with those of the reference test. Figure 7 shows that the experimental points roughly follow a linear relationship, corresponding to that proposed by Sines, which also passes through the point representing the reference test, and corresponding to the absence of residual stresses.

For the case of ground test specimens two straight lines are obtained, one representing the intrinsic behaviour for steel (longitudinal grinding with respect to the test specimen axis) and the other corresponding to the effect of surface finish (transverse grinding).

Therefore, the Sines criterion seems to take good account of the relationship which exists between residual stresses and the fatigue limit. Here, the introduc-

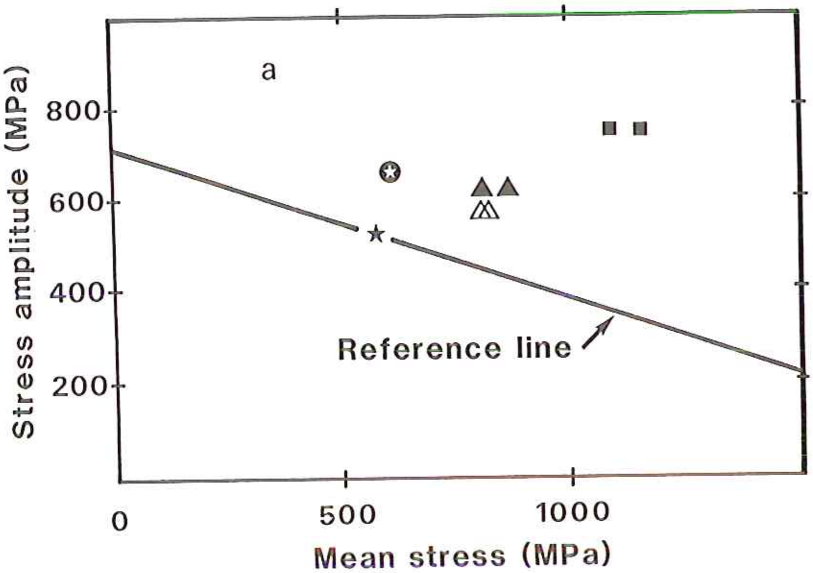

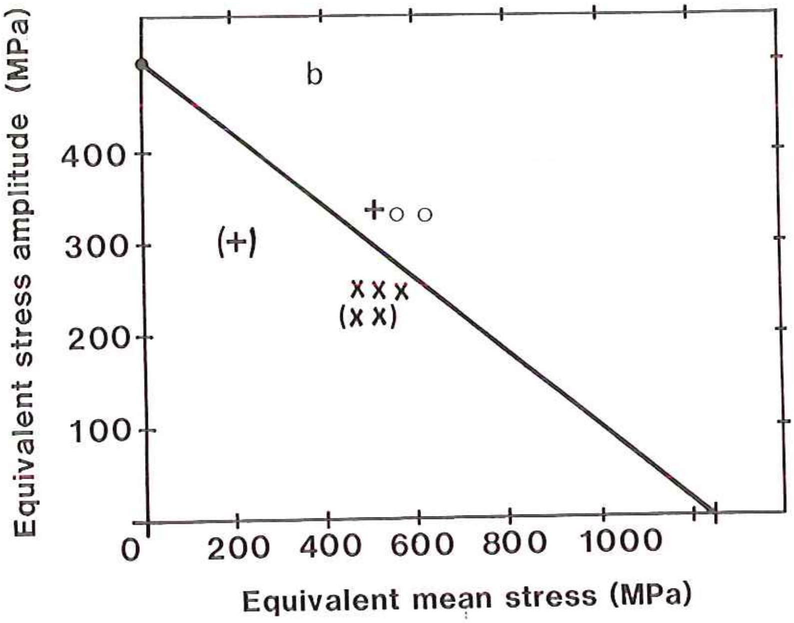

Fig 6 Experimental results interpreted using Kiocecioglu's criterion compared with the reference Haigh diagram: (a) induction hardened cylindrical bars (XC42 steel); (b) ground material (42CD4 steel)

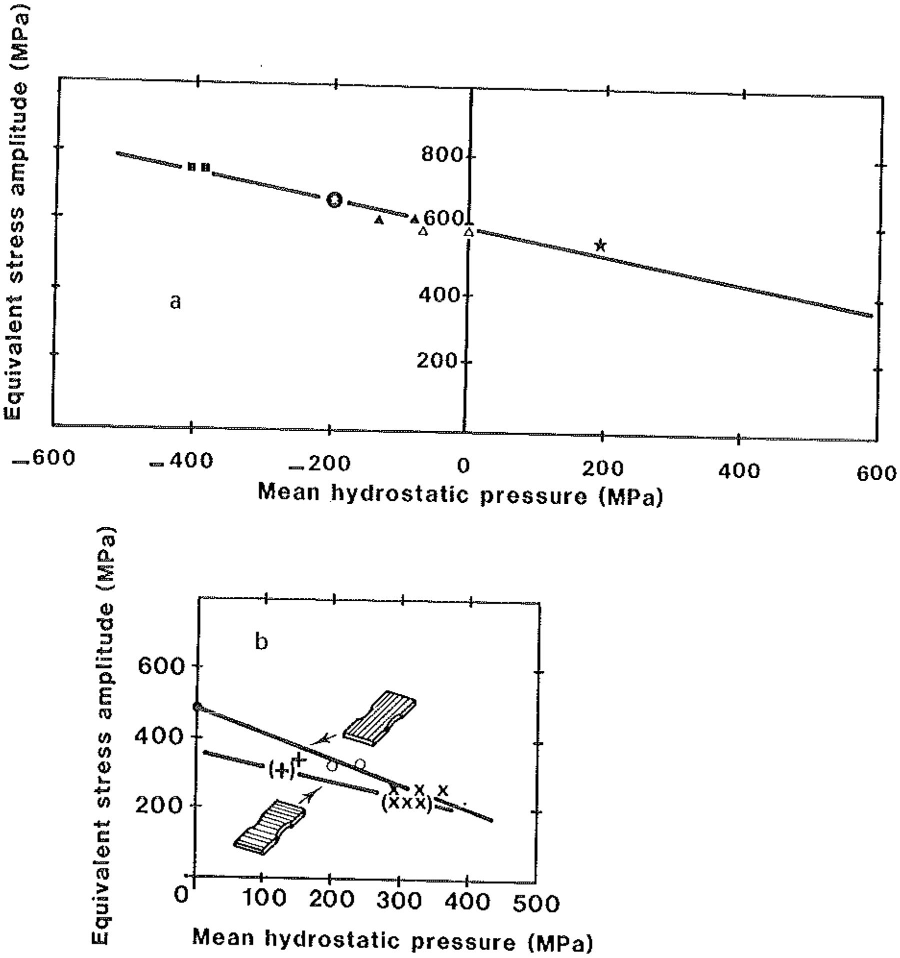

Fig 7 Experimental results interpreted using Sines' criterion: (a) induction hardened cylindrical bars (XC42 steel); (b) ground material (42CD4 steel)

tion of the hydrostatic pressure as one of the criterion's parameters appears to be fully justified.

The Crossland criterion

Crossland (9) has suggested a criterion close to that of Sines but in which the maximum hydrostatic pressure is considered, and not the mean value. The criterion is written

$$\tau_{oct,a} + \alpha \cdot \sigma_{oct,max} = \beta \tag{11}$$

If, as previously, the von Mises equivalent stress and the hydrostatic pressure, p_{max}, are used, then equation (11) becomes

$$\sigma_{equ,a} + \alpha' \cdot p_{max} = \beta \tag{12}$$

The maximum hydrostatic pressure is equal to one third of the sum of all the main stresses acting on the material at the maximum fatigue load. For example, in the case of plane bending tests on cylindrical specimens, one obtains

$$p_{max} = \frac{\sigma_a + \sigma_m + \sigma_{Rl} + \sigma_{Rt}}{3} \tag{13}$$

Using the maximum hydrostatic pressure, instead of the mean hydrostatic pressure, provides the means of differentiating between the loads to which the material is actually subjected and, in particular, between torsional fatigue tests and tensile or bending fatigue tests.

The results obtained using Crossland's criterion are plotted in Fig. 8. As in the case for Sines' criterion, the linear correlation of the results obtained by experiment is quite good. By comparing Figs 7(a) and 8(a), it can be seen that the Sines and Crossland criteria give slightly different values for the stress in pure alternating torsion, that is for p_m or $p_{max} = 0$. It follows that, for a conclusion regarding the validity of one or other of these two criteria, it would have been necessary to have had available the fatigue limit in pure alternating torsion.

The Sines and Crossland criteria, therefore, seem to agree well with the results obtained by experiment. The amplitdue of octahedral shear and the hydrostatic pressure appear to be useful parameters for describing the behaviour of a material subjected to multiaxial stresses.

The Findley–Matake criterion

Compared with the Sines and Crossland criteria, which consider the amplitude of shear acting on the plane of octahedral shear, Findley (**10**) and Matake (**11**) have proposed a criterion for which the main parameter is the amplitude of shear, τ_a, on the plane of maximum shear, and a second parameter, σ_n, acting perpendicular to this plane. The authors propose a criterion expressed as a limit curve of the form

$$\tau_a + \alpha \cdot \sigma_n = \beta \tag{14}$$

In the case of plane bending fatigue tests, the plane of maximum shear is inclined at 45 degrees with respect to the directions of the fatigue stresses, and perpendicular to the specimen surface. The values of τ_a and σ_n are calculated from the equations below, which are derived from Mohr's circle

$$\tau_a = \sigma_a/2 \tag{15}$$

$$\sigma_n = (\sigma_a + \sigma_m + \sigma_R)/2 \tag{16}$$

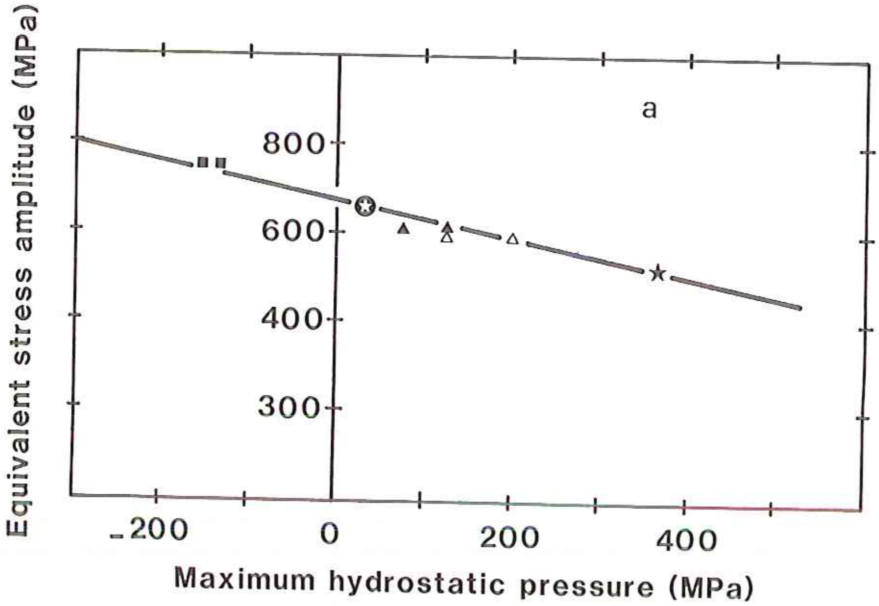

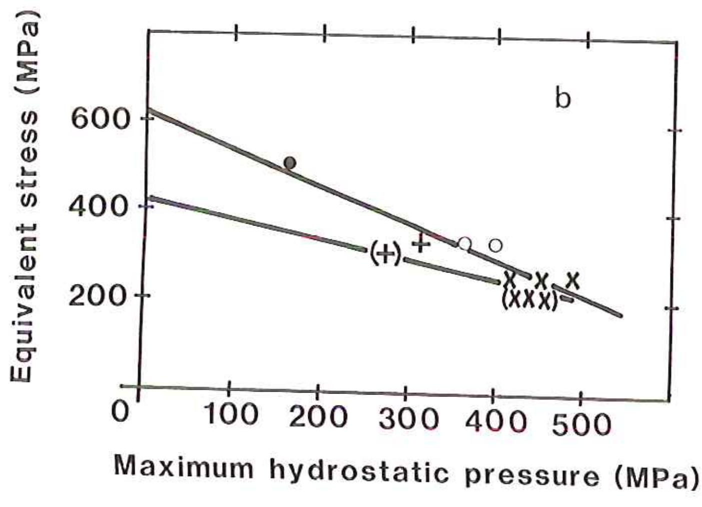

Fig 8 Experimental results interpreted using Crossland's criterion: (a) induction hardened cylindrical bars (XC42 steel); (b) ground material (42CD4 steel)

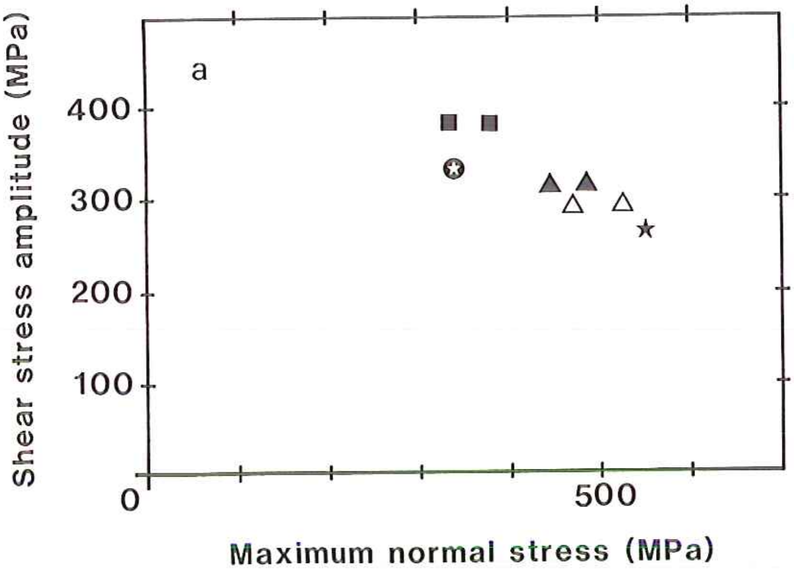

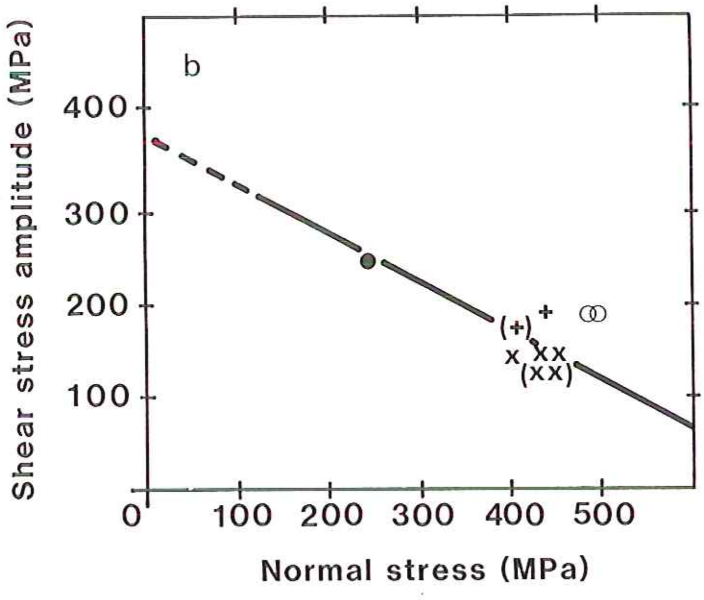

Fig 9 Experimental results interpreted using Findley and Mitake's criterion: (a) induction hardened cylindrical bars (XC42 steel); (b) ground material (42CD4 steel)

The results obtained by application of this criterion are plotted on Fig. 9, but these do not provide a clear correlation between the points obtained by experiment and those corresponding to the linear equation proposed. Further, the linear extrapolation for alternating torsion ($\sigma_n = 0$) gives rise to values for the alternating torsion fatigue limit which are much too high (Fig. 9(a)). Finally, in the case of the results for grinding, this criterion does not provide for any separation of the effects of surface roughness (Fig. 8(b)).

The Dang Van criterion

Dang Van (**12**) has put forward a criterion which brings into play local variables for the stabilised state. For the fatigue tests having a constant amplitude considered here, these variables are τ_a (the shear amplitude acting on the plane of maximum shear) and p_{max} (the maximum hydrostatic pressure).

The limiting curve for this criterion is given by the linear equation

$$\tau_a + \alpha \cdot p_{max} = \beta \qquad (17)$$

This criterion is close to that of Crossland. For simple bending fatigue tests, where σ_a is the tensile stress amplitude, we obtain

$$\tau_a = 1/2 \cdot \sigma_a \qquad \text{for the Dang Van criterion}$$

$$\tau_{oct,a} = \frac{\sqrt{2}}{3} \cdot \sigma_a \qquad \text{for the Crossland criterion}$$

The results obtained using the Dang Van criterion are plotted in Fig. 10. As for the Sines and Crossland criteria, we obtain a good correlation of the experimental points along a line passing through the point corresponding to the reference test $\sigma_m = 0$. Considering the results from the ground specimens, this criterion allows for the effect of roughness due to transverse grinding to be clearly distinguished, Fig. 10(b). A chart which plots a function of roughness, as shown in Fig. 11 for Dang Van's criterion, would be very useful for the engineers who want to take into account both residual stresses and surface roughness effects in fatigue calculations.

Conclusions

A number of multiaxial fatigue criteria have been compared utilizing results from fatigue tests and measurements of residual stresses on induction-hardened XC42 steel cylindrical specimens and on flat ground 42CD4 steel specimens. These comparisons allow the following conclusions to be drawn.

(1) The application of the Haigh or Goodman fatigue charts which neglect transverse residual stresses cannot be generalised. The use of this simplified method is subject to prior validation by experiment.

(2) The von Mises or Kiocecioglu criterion is not in any way able to account for true fatigue behaviour, where mean or residual stresses are present.

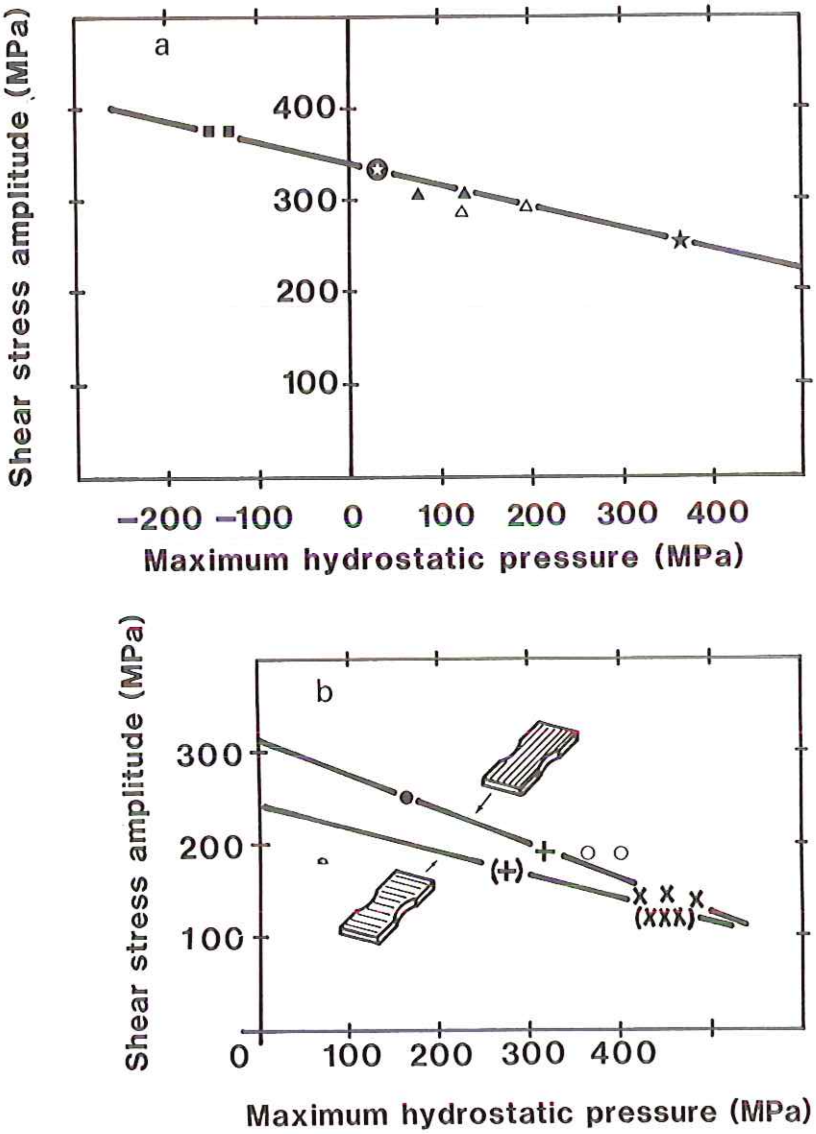

Fig 10 Experimental results interpreted using Dang Van's criterion: (a) induction hardened cylindrical bars (XC42 steel); (b) ground material (42CD4 steel)

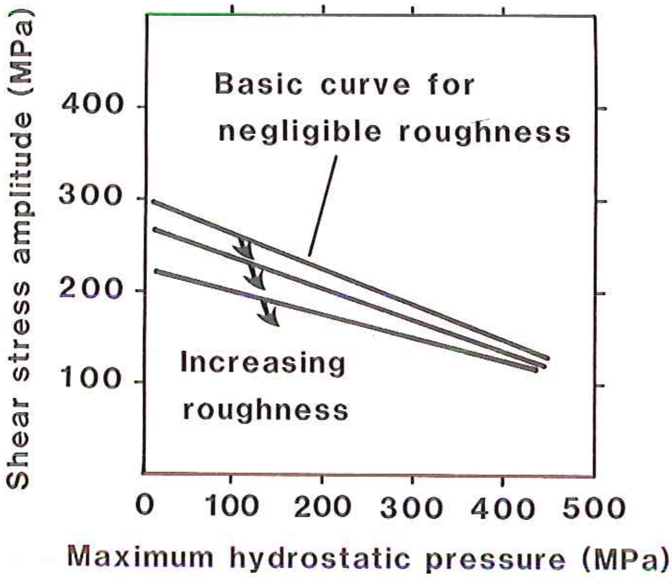

Fig 11 Plotting of Dang Van's chart for different values of roughness

The application of this criterion can only be justified in the case of purely alternating multiaxial stresses.

(3) The Sines, Crossland, and Dang Van criteria, which provide for the effect of hydrostatic pressure, appear to give a good explanation of experimental results. Further tests, in pure alternating shear (torsion) in particular, would no doubt provide the means of a more precise comparison between these three criteria.

(4) Comparison with the Findley–Matake criterion shows that fatigue strength depends more on hydrostatic pressure than on the stress perpendicular to the plane of maximum shear.

(5) For engineering components which are subject to simple fatigue loads, the Sines, Crossland, and Dang Van criteria appear to be able to estimate fatigue strength where residual stresses or surface roughness are present, provided that the phenomena of relief of fatigue stresses are taken into account. Dang Van's criterion would be more interesting, because it is applicable to out-of-phase multiaxial loading.

(6) To validate these criteria for other materials, or for other manufacturing processes which give rise to residual stress, and for fatigue loads of a more complex nature, additional tests are required.

References

(1) LEMAITRE, R., LEBRUN, J. L., and MAEDER, J. (1982) Contraintes résiduelles et fatigue, *Matériaux Techniques*, **9–10**, 297–305.

(2) SYREN, B., WOLFART, H., and MACHERAUGH, E. (1976) The influence of residual stress and surface topography on bending fatigue strength of machined Ck 25, in different heat treatment conditions, *Proc. 2nd Int. Conf. on Mech. Behaviour of Materials (Boston)*, pp. 212–235.

(3) KOIBUCHI, K., HAYAMA, T., and KAWAI, S. (1981) Residual stress and fatigue strength of surface hardened components, *1ère Conf. Internationale sur le Grenaillage de Précontrainte (Paris)*, Pergamon Press, Oxford, pp. 413–419.

(4) WOHLFAHRT, H. (1978) Influence of the residual stress on fatigue strength of steel, *Verlag Stahleisen MBH*, pp. 141–164.

(5) CHABENAT, A. and FLAVENOT, J. F. Mesure des contraintes résiduelles sur des axes trempés après chauffage par induction, *Traitement Thermique/Revue de Métallurgie*, 124–178, 233–239.

(6) SKALLI, N. and FLAVENOT, J. F. (1981) Influence des conditions de rectification sur les contraintes résiduelles introduites dans un acier 42CD4, *CETIM-Informations*, pp. 71, 58–65.

(7) KIOCECIOGLU, D., STULTZ, J. D., and NOFL, C. F. Jr (1975) Fatigue reliability with notch effects for AISI 4130 and 1038 steels, *Trans J. Engng Ind.*, **97**, 359–370.

(8) SINES, G. (1981) Fatigue criteria under combined stresses or strains, *J. Engng Mater. Technol.*, **13**, 82–90.

(9) CROSSLAND, B. (1956) Effect of large hydrostatic pressures on the torsional fatigue strength of an alloy steel, *Proceedings International Conference on the fatigue of metals*, Institution of Mechanical Engineers, London, pp. 138–149.

(10) FINDLEY, W. N. (1959) A theory of the effect of mean stress on fatigue of metals under combined torsion and axial load or bending, *J. Engng Ind.*, **81**, 301–306.

(11) MATAKE, T. and IMAI, Y. (1980) Fatigue interion for notched or unnotched specimens under combined stress state, *Z. AIRYO*, **29**, 993–997.

(12) KY DANG VAN (1973) Sur la résistance à la fatigue des métaux, *Sciences Techniques Armement*, **47**, 641–722.